Multicolor solitons due to four-wave mixing

Paul B. Lundquist and David R. Andersen
Department of Electrical and Computer Engineering, The University of Iowa, Iowa City, Iowa 52242

Yuri S. Kivshar
Optical Sciences Centre, Research School of Physical Sciences and Engineering, The Australian National University, 0200 Canberra, Australian Capital Territory, Australia

(Received 31 December 1996; revised manuscript received 21 April 1997)

The structure and stability of different types of multicolor optical spatial solitary waves created by interaction of light at a central frequency with two sideband waves both through cross-phase modulation and parametric four-wave mixing is presented. It is shown that a novel type of *three-color spatial soliton* appears above a power threshold when parametric coupling generates an instability of two-frequency solitary waves. [S1063-651X(98)04303-7]

PACS number(s): 42.65.Tg

Sky-rocketing network traffic and demand for greater data throughout has made soliton-based fiber-optics systems the clear choice for por tions of the future communications infrastructure [1]. To take full advantage of increases in transmission rates it will be necessary to develop equally fast all-optical switching devices suitable for wavelength-division multiplexing (WDM) systems. One proposed class of such devices is based on the reconfigurable multiport soliton crossbar switch operating with multifrequency spatial optical solitons: Solitons at one frequency act as steerable waveguides for data transmissions at other frequencies.

In Kerr (cubic or $X^{(3)}$) media, two-component (or two-color) solitons have been investigated under the primary assumption that four-wave mixing (FWM) is neglected, in the context of pulse propagation in optical fibers and beam propagation in slab waveguides (see, e.g., Refs. [2,3]). However, the third-order nonlinear susceptibility that supports solitary waves in Kerr media can lead simultaneously (subject to phase-matching conditions) to a FWM process in which two photons in a central frequency field are converted into one photon in each of two sideband fields (and *vice versa*) [4]. Some special sech-like solitary waves in the presence of FWM have been already found by direct substitution [4–6]. However, general families of multicolor solitary in the presence of FWM interaction have not been investigated yet. In this paper, we analyze, for the first time to our knowledge, different types of solitary waves in the problem of degenerate FWM interaction considering the case of spatial self-trapping in a slab waveguide. In particular, we show that above a certain power threshold the FWM interaction leads to *an instability of two color solitons* and, instead, there appears a novel type of stable stationary localized waves, *three-color optical solitons*, in which parametric wave mixing is exactly balanced by the nonlinear effect of self- and cross-phase modulation. This resembles the self-trapping mechanism by which solitary waves are possible due solely to parametric wave coupling in a quadratic nonlinear medium [7], and therefore the multicolor solitons described in this paper can be regarded as a unique class of three-wave parametric solitary waves supported by a combined action of self-induced modulation, cross-phase modulation, and FWM parametric coupling between the field envelopes corresponding to different carrier frequencies.

Several novel applications may result from the FWM solitons. First, in a crossbar switch based on the collision properties of spatial solitons, it may be possible to use the FWM interaction to provide parametric amplification in one of the frequency components. Second, there have also been a number of suggestions for logic devices based on soliton collision-induced phase shifts [8]. These devices can be realized by employing the collisional shifts in the frequency composition of FWM spatial solitons. Finally, in a temporal soliton context, multifrequency pulses similar to those described here may be produced by using a parametric soliton laser with a dispersion-shifted fiber [9].

We start our analysis by considering the spatial analog of the standard four-wave mixing process and introducing three envelope functions $\phi_j(x,z)$, where $j=a,b,c$ for an electric field,

$$E(x,z;t)=E_0\{\phi_a+\phi_b e^{-i\delta\omega t}+\phi_c e^{i\delta\omega t}\}e^{-i\omega t}+\text{c.c.}, \quad (1)$$

where c.c. stands for the complex conjugate values, $\delta\omega$ is the side-band frequency shift, so that the central frequency and two side-band frequencies are taken as ω, $(\omega+\delta\omega)$, and $(\omega-\delta\omega)$, respectively. These different frequency components of the field interact due to the cubic (or $X^{(3)}$) nonlinear response of the Kerr-type optical medium. It is assumed that the phase matching conditions are satisfied for the main frequency and the side-band frequencies only, whereas the interaction of these three waves of other frequencies and their combinations is incoherent and, therefore, generation of additional frequency components can be neglected. Substituting Eq. (1) into the nonlinear scalar wave equation yields a set of three coupled nonlinear (Helmholtz-type) equations:

$$\nabla^2\phi_a+\beta_a^2\phi_a+\gamma_a[\phi_a(|\phi_a|^2+2|\phi_b|^2+2|\phi_c|^2)+2\phi_a^*\phi_b\phi_c]=0,$$

$$\nabla^2\phi_b+\beta_b^2\phi_b+\gamma_b[\phi_b(2|\phi_a|^2+|\phi_b|^2+2|\phi_c|^2)+\phi_a^2\phi_c^*]=0, \quad (2)$$

$$\nabla^2\phi_c+\beta_c^2\phi_c+\gamma_c[\phi_c(2|\phi_a|^2+2|\phi_b|^2+|\phi_c|^2)+\phi_a^2\phi_b^*]=0,$$

where $\gamma_j=\beta_j^2 n_{2j}/n_j$ for $j=a,b,c$; n_{2a}, n_{2a}, and n_{2c} are the nonlinear susceptibilities; n_a, n_b, and n_c are the linear refractive indices; and β_a, β_b, and β_c for *linear* propagation constants. The field labeled by the subscript ''*a*'' is the beam with the central frequency ω, whereas the other two fields, the beams ''*b*'' and ''*c*'', are characterized by the sideband frequencies $(\omega+\delta\omega)$ and $(\omega-\delta\omega)$, respectively. All fields are normalized by the strength of the nonlinearity. The last term in each of these equations describes phase-matched parametric FWM interaction between the fields.

Neglecting the parametric FWM interaction is usually justified by the argument that the dispersion leads to rapid oscillations in the phase mismatch [2]. Indeed, for small nonlinear phase modulations in the fields, the FWM term of each field experiences a phase rotation $e^{\pm i\Delta z}$ relative to the field where the linear propagation mismatch is defined as $\Delta=2\beta_a-\beta_b-\beta_c$.

This argument is no longer valid for small values of Δ or for powers sufficient to produce a nonlinearity-induced change in the refractive index comparable to the linear mismatch. In such a case, the nonlinear phase modulation provides shifts in the propagation constants that are sufficient to exactly balance the linear phase mismatch making the phases of the FWM terms stationary relative to the fields. To find these self-trapped stationary states, we look for solutions of the nonlinear Helmholtz equations (2) in the standard form

$$\phi_a(x,z)=U(x)e^{i(k_a z+\theta_a)},$$

$$\phi_b(x,z)=V(x)e^{i(k_b z+\theta_b)}, \tag{3}$$

$$\phi_c(x,z)=W(x)e^{i(k_c z+\theta_c)},$$

where U, V, and W are the real amplitudes of the fields; θ_a, θ_b, and θ_c are absolute (initial) phases of the fields; and a set of *effective* propagation constants k_a, k_b, and k_c is produced by nonlinear self- and cross-phase modulation.

Stationary wave propagation can be achieved provided both the effective propagation constants and the absolute phases are matched. The corresponding phase-matching condition for the effective propagation constants, $2k_a=k_b+k_c$, describes a surface in the space of the three effective propagation constants that may be parametrized as follows: $k_a=Q$, $k_b=Q+R$, and $k_c=Q-R$. It should also be noticed that the absolute phase mismatch defined as $\Delta\theta=2\theta_a-\theta_b-\theta_c$ can only be 0 or π for coupled multifrequency stationary waves, because all other absolute phase mismatches lead to a complex valued polarization in the nonlinear Helmholtz equations.

A set of coupled ordinary differential equations results from substituting Eqs. (3) into Eqs. (2). Stationary field profiles can then be found numerically at any fixed choice of the parameters Q and R (see Ref. [10]) with appropriate boundary conditions: namely, for bright solitary waves we analyze in this paper, ϕ_i and $\partial\phi_i/\partial_x$ should vanish at a distance sufficiently far from the soliton center so that errors are negligible. For the examples presented in this paper, the following parameters were chosen: $\delta\omega/\omega=0.01$, $\beta_a=1.0$, $\beta_b=1.212$, $\beta_c=0.891$, $\gamma_a=1.0$, $\gamma_b=1.2242$, $\gamma_c=0.88209$. These linear propagation constants result in a large propagation mismatch of -0.103.

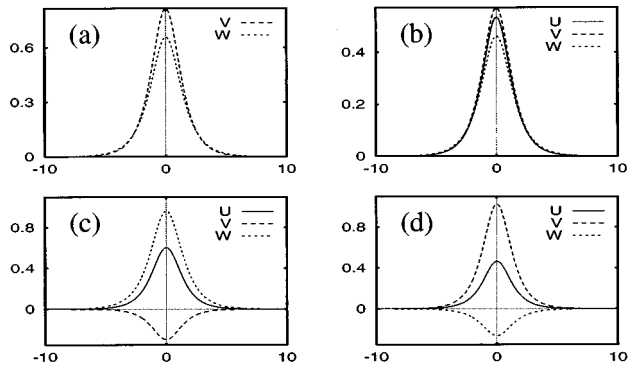

FIG. 1. Profiles of stationary solutions (3) for $Q=1.4$, and $R=0.1605$. Field amplitude and position variables are normalized (dimensionless) as defined in the text. (a) Two-color soliton. (b) Three-color soliton with the zero absolute phase mismatch, σ soliton. (c), (d) Two examples of three-color solitons with a π absolute phase mismatch, $\pi-$ and $\pi+$ solitons.

One-color solitary waves are precisely the well-known sech-type solutions of the cubic nonlinear Schrödinger (NLS) equation. They can be immediately obtained from Eqs. (2) assuming that only one field, ϕ_a, ϕ_b, or ϕ_c, is nonzero whereas two others vanish. Unlike these one-color localized waves, multicolor solitary waves appear as mutually coupled states of two or three different frequencies. Figure 1 illustrates some examples of two- and three-color stationary states for $Q=1.4$ and $R=0.1605$.

Two-color solitary waves can exist as stationary localized solutions only when the field component with the central frequency ω exactly vanishes (i.e., when $\phi_a=0$). Then, the FWM coupling in the polarization vanishes as well so that no additional frequencies are generated. The similar kind of two-frequency solitons, mutually coupled only due to the cross-phase incoherent interaction, have been discussed in previous works (see, e.g., [2,3]) and one of the examples is illustrated in Fig. 1(a).

Three-color solitary waves include the effect of FWM coupling and therefore the phase-matched parametric interaction between the frequencies become important. In an earlier paper [5], this type of solution was found by a direct substitution of the familiar sech-type profiles deriving a set of conditions for other parameters. Such exact analytical solutions allow one to describe only very special localized modes and sometimes they give incomplete or even wrong results. As an example, we mention the recent work by Sammut *et al.* [11] where it was found, in particular, that the sech-type solutions earlier obtained for the problem of the third-harmonic generation [5] correspond to degenerate absolutely unstable multihump solitary waves. Therefore, these exact solutions may not provide useful information about self-trapping of the fundamental beams due to FWM interaction.

To describe the complete families of the localized solutions for the FWM-coupled solitary waves, we solve the system of three coupled equations for the real functions $U(x)$, $V(x)$, and $W(x)$. Bright solitons with vanishing asymptotics

at infinity correspond to separatrix solutions homoclinic to zero. We find such solutions numerically for values of Q and R. As a result, we reveal that three-color solitary waves can exist of three distinct types, and they can be classified by two possible absolute phase mismatches. Wave profiles illustrated in Figs. 1(c) and 1(d) correspond to the case where the absolute phase mismatch $\Delta\theta$ is equal to π (this is indicated in the figures by showing negative field amplitudes). If the linear and nonlinear susceptibilities for the two sidebands were identical for the two sidebands then there would be a symmetry corresponding to exchange of the sideband field profiles. Parametric interaction destroys this symmetry and accounts for the slight difference between the two sets of field profiles. In the soliton shown in Fig. 1(c) the amplitude of the central frequency beam is slightly larger than that of the soliton shown in Fig. 1(d). We shall use the following naming scheme for stationary waves with a π absolute phase mismatch: if more power is in the ϕ_b field than in the ϕ_c field we call this state a $\pi+$ solitons, but if the sideband field powers have the opposite ordering then we call it a $\pi-$ soliton. The third type of the three-color solitary wave is illustrated in Fig. 1(b). In this stationary state the total absolute phase mismatch is zero, $\delta\theta=0$. To distinguish this third soliton from the $\pi+$ and $\pi-$ solitons we will refer to this type as a σ soliton.

Because the two- and three-color solitary waves are characterized by two independent parameters Q and R, their stability is not a trivial issue. Analysis of the stability of multiparameter solitary waves has begun only recently (see, e.g., [12,13]), and many issues still remain to be understood. Here we demonstrate the stability of σ solitons employing the approach based on catastrophe theory (see, e.g., Ref. [14] for a general review). This approach has been recently generalized to a three-wave mixing interaction where solitary wave families are described by two-parameter invariant surfaces [13], and involves the analysis of the system Hamiltonian as a function of two additional conserved quantities resulting from the symmetries according to Noether's theorem.

First, we define the conserved quantities of our model. The system Hamiltonian results from translational invariance of Eqs. (2) along the propagation direction z,

$$H=\int_{-\infty}^{\infty}\left\{\sum_j\left[-\gamma_j|\pi_j|^2+\frac{1}{\gamma_j}\left|\frac{\partial}{\partial x}\phi_j\right|^2-\frac{\beta_j^2}{\gamma_j}|\phi_j|^2-\sum_{j\neq k}|\phi_j|^2|\phi_k|^2-\frac{1}{2}|\phi_j|^4\right]-(\phi_a^{*2}\phi_b\phi_c+\phi_a^2\phi_b^*\phi_c^*)\right\}dx, \qquad (4)$$

where $\pi_j=-\gamma_j^{-1}(\partial/\partial z)\phi_j$ are the canonical field momenta and $j=a,b,c$.

There also exist two internal symmetries that lead to conserved quantities. An equal variation in the absolute phases of all three fields leaves the set of nonlinear Helmholtz equations unchanged. This symmetry generates the conservation of *total power*. The total power is simply the sum of the partial powers calculated for each of the fields: $P=\Sigma_j P_j$, where $P_j=i\int_{-\infty}^{\infty}\{\phi_j^*\pi_j-\text{c.c.}\}dx$, for $j=a,b,c$.

Because parametric coupling due to the FWM effect allows coherent interaction and energy transfer between the fields, the powers of each individual field are not conserved. However, a second conserved power results from the invariance of the Hamiltonian when the phases of the two sideband fields are varied in the opposite directions. This symmetry leads to the conservation of the so-called *skew power* $S=P_b-P_c$.

The conservation of these two power invariants has a simple physical meaning based on an analogy with quantum optics. Indeed, every photon taken out of the central frequency field must correspond to a photon added to each of the sidebands (and *vice versa*). This type of parametric coupling permits only a constant photon number difference between the two sidebands. Thus the power in the two sidebands is expected to change in tandem over any propagation distance. Accompanying these power changes in the sidebands, a compensating variation in the central frequency power leads to a constant net power.

To analyze the solution stability we use a Hamiltonian in a rotating frame so that the transverse profiles are stationary solutions. From the canonical equations it is easy to show that this new Hamiltonian is given by $J=H+QP+RS$. This rotating-frame Hamiltonian can also be viewed as a Lyapunov function in which Q and R play the role of Lagrange multipliers [15] (see also Refs. [13,14] for other examples). The stationary solutions then correspond to extrema or saddle points of this Lyapunov function: $\delta J=0$. Stable solutions are global extrema of the Lyapunov function for which growth of any perturbation violates conservation laws. If the Hamiltonian is bounded from below, then it follows that the stationary solution with the lowest value of Hamiltonian for a constant pair of P and S is stable.

In Fig. 2, we illustrate several Hamiltonian surfaces as a function of the power P and skew power S as viewed from $H\to-\infty$. For low powers, the two-color solutions indicated by the label BC are stable. For powers sufficient to balance the phase mismatch with nonlinear phase modulation, the

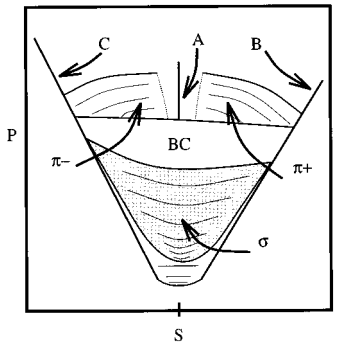

FIG. 2. Schematic of normalized Hamiltonian surfaces for stationary waves as a function of P and S viewed from $H\to-\infty$.

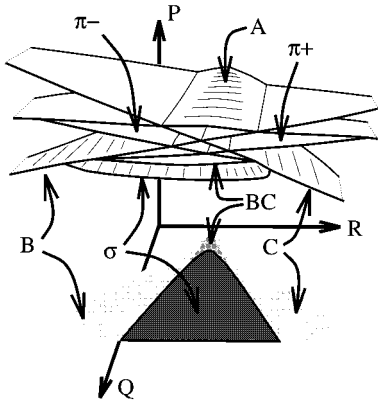

FIG. 3. Power surfaces for stationary waves as a function of normalized variables Q and R. The near cross section of the surfaces correspond to $Q=1.4$ and the parameters are the same as in Fig. 1.

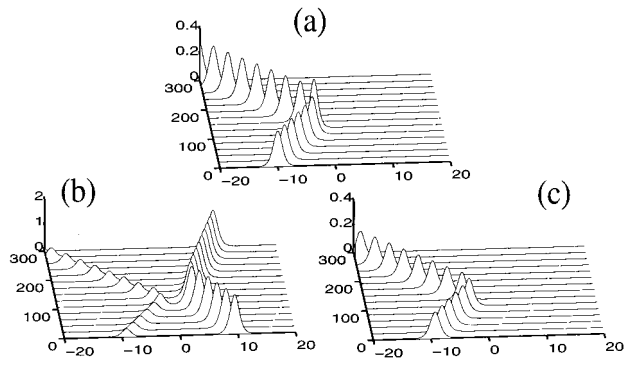

FIG. 4. Collision between a σ soliton and a one-color soliton in the upshifted sideband: Intensities $|\phi_j|^2$, where $j=a,b,c$, are shown in (a), (b), and (c), respectively. Field amplitude and position variables are normalized as defined in the text.

three-color σ solitons exist as a lower branch from a bifurcation of the two-color solutions. At powers above this bifurcation curve, the σ solitons are stable whereas the two-color solitons become unstable. The two one-color sideband waves are illustrated as lines and are labeled B and C. These one-parameter solutions are always stable and satisfy one of the conditions, $P=S$ or $P=-S$. Near the top of Fig. 2, the two-color and σ soliton surfaces are cut away, revealing the π soliton surfaces and the central frequency one-color line labeled A. These three-color $\pi+$ and $\pi-$ waves are always unstable. The two π solutions approach the one-color central frequency wave for low skew powers.

Because coupling between waves with identical propagation constants leads to radiation and a reduction in the power integral, it is useful to see how the powers of different types of waves relate as a function of Q and R. Power surfaces for the seven solution types are illustrated in Fig. 3. A ''shadow'' of the stable power surfaces is shown in the $P=0$ plane, where bifurcation between the two-color and σ solitons occurs along the line separating the two shaded regions. In this diagram, the one-color solutions appear as surfaces because each solution profile maps to a line. For example, the central frequency surface is independent of R. It should be noted that because the skew-power and Hamiltonian information is missing in this diagram, most of the intersections between power surfaces do not correspond to bifurcations. Bifurcations correspond only to lines where solution surfaces begin or end.

General properties and stability of all types of bright multicolor solitons can be confirmed by beam propagation, numerically integrating the nonlinear coupled equations (2) in the paraxial approximation, when the system is reduced to three NLS-type equations coupled through cross-phase modulation and FWM interactions. Such an approximation is well known and it is based on the fact that all envelope functions vary slowly along the propagation direction z. In numerical simulations, we have found that one-color sideband solitons, two-color solitons *below* the power threshold, and three-color σ solitons are all stable. However, the one-color central frequency stationary soliton, the three-color π solitons, and the two-color solitons *above* the σ wave power threshold were all found to be unstable. These results are in full agreement with the analysis of the invariant surfaces, as we described above. We tested each stationary wave type for the parameters $Q=1.4$ and $R=0.1605$ by running a numerical beam propagation from a perturbed initial condition over distances as great as 1500 normalized length units (both amplitude and phase perturbations were applied). This corresponds to about 24 full cycles in the linear phase mismatch. We also monitored the conserved total and skew powers during the simulations to assure that the step sizes were selected correctly.

To confirm further the stability of the FWM solitons and observe their robustness under large-amplitude perturbations, we numerically investigated collisions between the solitary waves of different types. As an example, in Fig. 4 we present intensities of the frequency components of the solitons for a collision between a three-color σ soliton and a one-color up-shifted sideband soliton corresponding to the parameters used in Fig. 1. The localized wave launched from the left had the initial field profile shown in Fig. 1(b) and the wave launched from the right was a one-color soliton in the upper sideband. The initial field profiles were chosen so that there was about 120 degrees phase difference between the two solitons. In spite of the fact that the model is not integrable, the solitary waves collide in a billiard-ball fashion preserving their identities.

In conclusion, we have described, for the first time to our knowledge, different families of multicolor bright spatial optical solitary waves in the problem of degenerate four-wave-mixing interaction. Bifurcations of invariant surfaces for the two-parameter FWM solitons as well as the stability properties of one-, two-, and three-color solitary waves reveal that two-color solitons become unstable above a certain power threshold and only three-color FWM solitons with zero absolute phase mismatch are stable. These three-color solitons present a novel class of mutually coupled stationary states for which the FWM interaction is exactly balanced by nonlinear phase modulation. Below the power threshold, two-color waves with no parametric coupling through FWM interaction are stable. One-color solitons in the sideband frequencies are stable, but one-color waves in the central

frequency always decay through the FWM parametric interaction. All the predictions based on the analysis of spatially localized stationary solutions and their invariant surfaces have been confirmed by direct numerical simulations.

P.B.L. acknowledges partial support from the Iowa Space Grant Consortium, and David R. Andersen acknowledges support from the Carver Foundation. They thank N. Akhmediev for useful conversations. Y.K. is a member of the Australian Photonics Cooperative Research Centre, and he is indebted to R. A. Sammut and A. V. Buryak for valuable discussions.

[1] A. Hasegawa and Y. Kodama, *Solitons in Optical Communications* (Oxford University Press, Oxford, 1995).

[2] C. R. Menyuk, J. Opt. Soc. Am. B **5**, 392 (1988); G. P. Agrawal, *ibid.* **7**, 1072 (1990); N. N. Akhmediev, A. V. Buryak, J. Soto-Crespo, and D. R. Andersen, *ibid.* **12**, 434 (1995).

[3] H. T. Tran and R. A. Sammut, Phys. Rev. A **52**, 3170 (1995).

[4] L. M. Kovachev and V. N. Serkin, Izv. Akad. Nauk Arm. SSR, Fiz. **53**, 1559 (1988); D. Liu and H. G. Winful, Opt. Lett. **16**, 67 (1991); L. M. Kovachev, Opt. Quantum Electron. **24**, 55 (1992); Y. Chen, and J. Atai, Opt. Lett. **19**, 1287 (1994).

[5] Y. Chen, Phys. Rev. A **50**, 5145 (1994).

[6] N. A. Ansari, R. A. Sammut, and H. T. Tran, J. Opt. Soc. Am. B **13**, 1419 (1996); **14**, 298 (1997).

[7] See, e.g., A. V. Buryak and Yu. S. Kivshar, Opt. Lett. **19**, 1612 (1994); Phys. Lett. A **197**, 407 (1995); and also the review paper G. I. Stegeman, D. J. Hagan, and L. Torner, Opt. Quantum Electron. **28**, 1691 (1996).

[8] D. R. Andersen and J. P. Robinson, Opt. Comput. Processing **2**, 57 (1992).

[9] K. Suzuki, M. Nakazawa, and H. Haus, Opt. Lett. **14**, 320 (1989).

[10] P. B. Lundquist and D. R. Andersen, J. Opt. Soc. Am. B **14**, 87 (1997).

[11] R. A. Sammut, A. V. Buryak, and Yu. S. Kivshar, Opt. Lett. **22**, 1385 (1997).

[12] A. V. Buryak, Yu. S. Kivshar, and S. Trillo, Phys. Rev. Lett. **77**, 5210 (1996).

[13] A. V. Buryak and Yu. S. Kivshar, Phys. Rev. Lett. **78**, 3286 (1997).

[14] F. V. Kusmartsev, Phys. Rep. **183**, 1 (1989).

[15] E. Kuznetsov, A. Rubenschik, and V. Zakharov, Phys. Rep. **142**, 103 (1986).